Spectroscopic Study of a Spectrally Sensitized Tabular Grain AgBr Emulsion Using Both AFM and PSTM Techniques

C. Pic*, D. Martin*, J. Guilment*, F. De Fornel†, J. P. Goudonnet‡

** Kodak European Research, Laboratoire d'Analyses, C.R.T. 60-3, F-71102 Chalon sur Saône, France*

†Laboratoire de Physique, Faculté des Sciences Mirande, Université de Bourgogne, BP 138, 21004 Dijon, France

‡Equipe d'Optique Submicronique, Laboratoire de Physique, Faculté des Sciences Mirande, Université de Bourgogne, BP 138, 21004 Dijon, France

The scope of this study was to correlate the topographic information provided by atomic force microscopy (AFM) with optical properties of the AgX tabular grain photographic emulsion samples collected with near-field optical microscopies. Images of spectrally sensitized AgBr tabular grains were performed, using both AFM and photon scanning tunneling microscopy (PSTM). PSTM images of spectrally sensitized AgBr microcrystals, recorded at various excitation wavelengths, showed an amplification of the apparent thickness of the grains when excited in the absorption range of the dye. This can be explained by the contribution of the fluorescence of the sensitizing dye to the measured signal in the PSTM. The increase of the PSTM response depended also on the dye coverage and on the stack of microcrystals. The visible absorption and fluorescence spectra of the spectrally sensitized emulsion obtained at room temperature at a macroscopic scale were in good agreement with the PSTM observations.

Journal of Imaging Science and Technology 42: 126–134 (1998)

Introduction

The intrinsic sensitivity of silver bromide emulsion is limited to blue and UV radiations. By the addition of sensitizing dyes, it becomes possible to increase the sensitivity of silver bromide grains to the entire visible range. The understanding and analysis of sensitizing dye adsorption mechanisms is of the highest interest for photographic science. Until now, different techniques were applied to collect both topographical and spectral information on the adsorption of dye molecules on the grains (J-aggregates). These techniques included low-temperature luminescence microscopy[1–4] or analytical color fluorescence electron microscopy (ACFEM).[5] However, low magnification of optical microscopy or use of a focused electron beam for the sample excitation instead of photons represented the main disadvantages of these techniques for the study of photosensitive materials.

New experimental approaches to high-resolution studies of sensitizing dyes exist now, using the near-field microscopies: scanning tunneling microscopy (STM), atomic force microscopy (AFM) or near-field optical microscopy. The AFM technique has the advantage of being able to image insulating surfaces. Several groups confirmed the ability of AFM to reach atomic resolution on silver halide grain surfaces.[6–8] In the first studies, the samples observed were ideal systems like silver bromide thin films or polished single crystals. This work was done to determine topographic characteristics of dye aggregates. Haefke et al.[9] presented the first AFM images of merocyanine dye islands vapor-deposited on an (001) oriented AgBr thin film. Their results were not related to the results obtained with standard sensitization methods.

Therefore, it was of the highest interest to study a practical system, because modern photographic films are actually elaborated systems, consisting mainly of silver halide grains with other organic components in a gelatine layer.

In recent publications, several authors studied a real system: conventional chemically and/or spectrally sensitized polydisperse emulsions.[10,11] AFM images of spectrally sensitized AgBr cubic grains with various surface coverages (10 or 40%) of thiacarbocyanine or oxacarbocyanine dye were obtained, which were in good agreement with the observations yielded by scanning electron microsocopy (SEM) or ACFEM methods.[5] Successful STM imaging of a monolayer of cyanine dye aggregates was possible by choosing a sample composed of a thin oriented Ag(111) film (150 nm high) vapor-deposited on a mica substrate.[12]

The near-field scanning optical microscopies (NSOM) are attractive methods for detecting optical properties of the sample in addition to the topographic information. A recent work[13] described investigations of tabular AgBr grains with NSOM equipment and the collection of fluorescence spectroscopy of the cyanine dye adsorbed on AgBr tabular grains.

In this article, we present another approach to near-field optical microscopy study of spectrally sensitized silver bromide microcrystals using both PSTM and AFM.

Experimental

The study was carried out on AgBr and AgBrI tabular grains (Fig. 1). The average diameter of the grains was 1.8 to 2.0 μm and the average thickness 0.130 μm. The grains

Original manuscript received March 6, 1997.

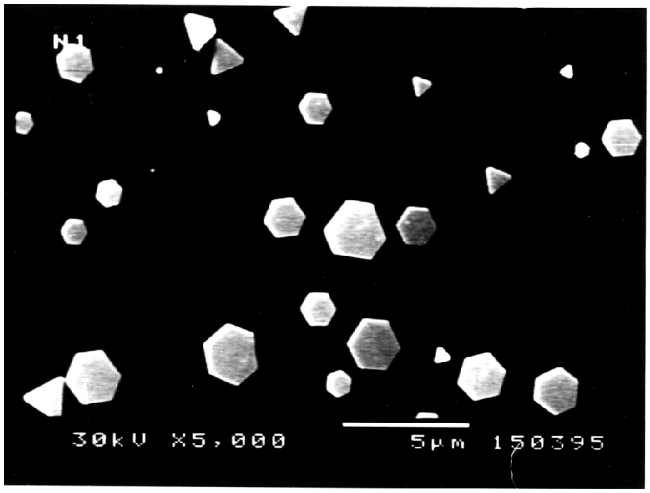

Figure 1. SEM image of a tabular grain emulsion coated on a glass substrate.

were washed and diluted with warm water (45°C) and then coated on glass substrate (5 × 5 mm) by ultracentrifugation at 70,000 rpm to obtain a rather uniform distribution of grains with a minimum of overlap. The gelatine was kept because it improved the quality of the sample preparation and did not perturb the quality of the images.

The sensitizing dye chosen belongs to the oxacarbocyanine class with the following formula:

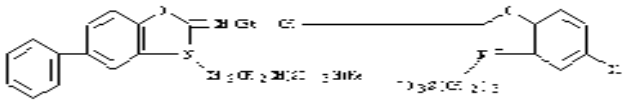

The dye was added to the grains under methanolic form and the dye coverage was estimated using UV-visible absorption spectroscopy to calculate Langmuir isotherm parameters for the dye-grain system.

The PSTM instrument was developed at the University of Dijon and was described in the Refs. 14, 15, and 16. As shown in Fig. 2, the sample was placed on a semicylindrical prism with an index matching gel between the prism and the sample. The classical source for such an instrument was a He–Ne laser, but the experiments were performed at various excitation wavelengths with a white light source.

The polychromatic light source was an ORIEL xenon lamp (with slits of 3.16 mm at the output of the monochromator that corresponded to a spectral bandwidth of 10 nm). In the following experiments, the probe tip detected simultaneously in the near-field the fluorescence and the excitation signals. The PSTM images were performed using the constant intensity mode of imaging and the feedback was realized on the intensity of the light detected by the optical fiber tip during the scanning. The distance between the tip and the sample surface was about 50 to 100 nm. The excitation intensity at the sample was close to 2 mW/cm^2.

A Nanoscope D3000 (Dimension 3000) from Digital Instruments, Santa Barbara, CA, was used to record the AFM images.

The comparison between PSTM and AFM pieces of information required a localization method. We succeeded in elaborating a special grid pattern intended for the spatial localization of tabular microcrystals on the surface of samples.

Results and Discussion

One of the characteristics of the sensitizing dyes is the reversible formation of dye aggregates[17–19]: dimers, trimers, and J-aggregates in organic solvents or adsorbed on silver halide microcrystals. The spectral feature associated with J-aggregates is a sharp and strong electronic transition significantly red-shifted from the molecular band of the monomeric form. The J-band has been attributed to close-packed dye molecules stacked plane-to-plane along the

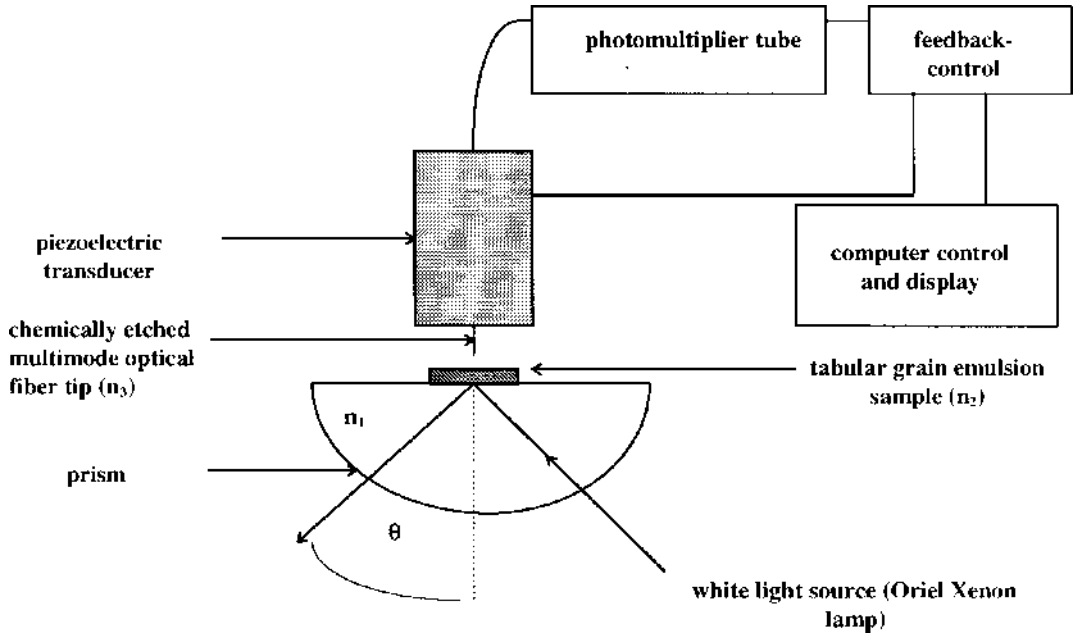

Figure 2. Schematic of the PSTM experimental setup.

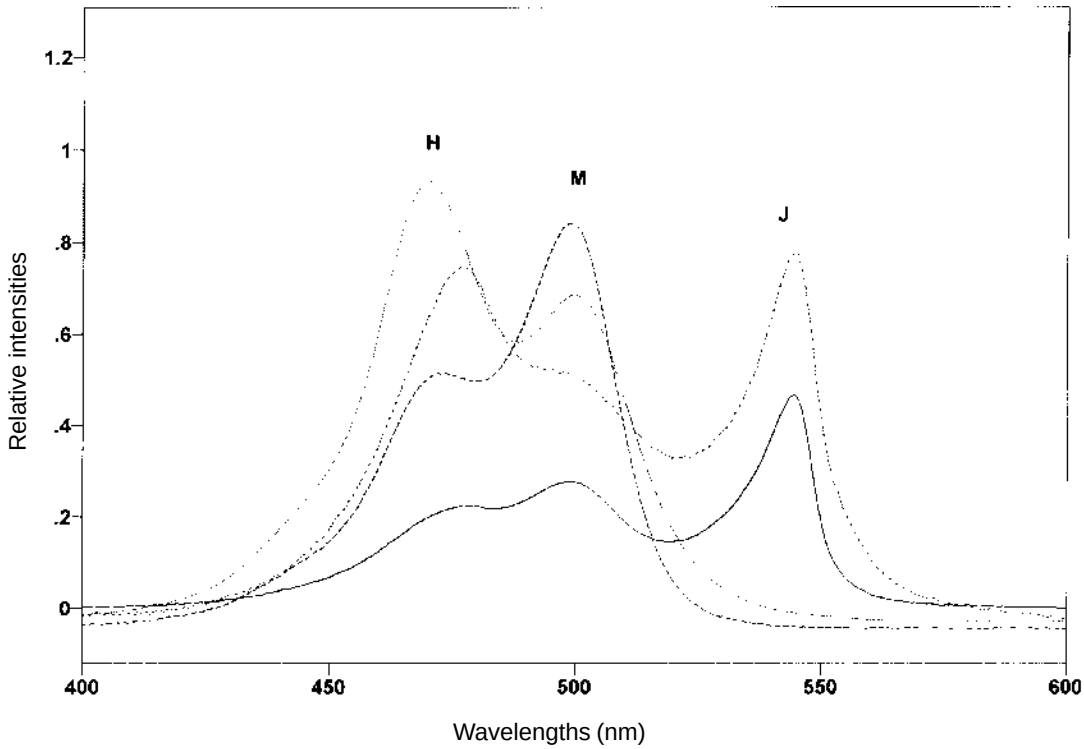

Figure 3. Visible absorption spectra of sensitizing dye dissolved in methanol, water or aqueous solution with Na_2SO_4. Curves M, H, and J correspond, respectively, to the dye under monomeric, H- or J-aggregate form: _____ dye 5.6 10^{-6} mol/L in water + Na_2SO_4 60 g/L, -.-.-.-.-. dye 5.6 10^{-6} mol/L in water + Na_2SO_4 100 g/L, – – – – dye 5.6 10^{-6} mol/L in methanol,..... dye 2.8 10^{-4} mol/L in water.

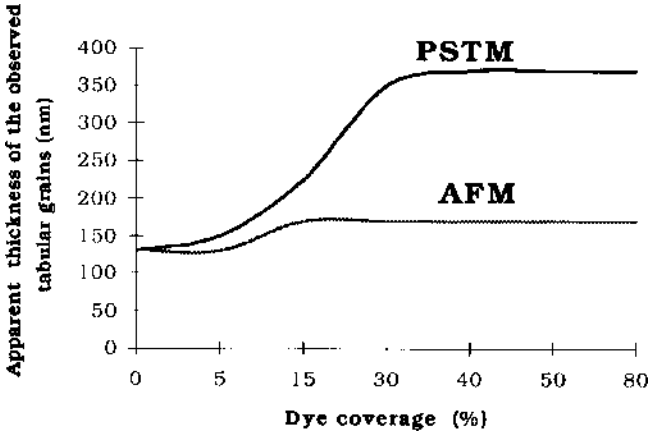

Figure 4. Evolution of the apparent thickness of the tabular grains observed with PSTM and AFM techniques.

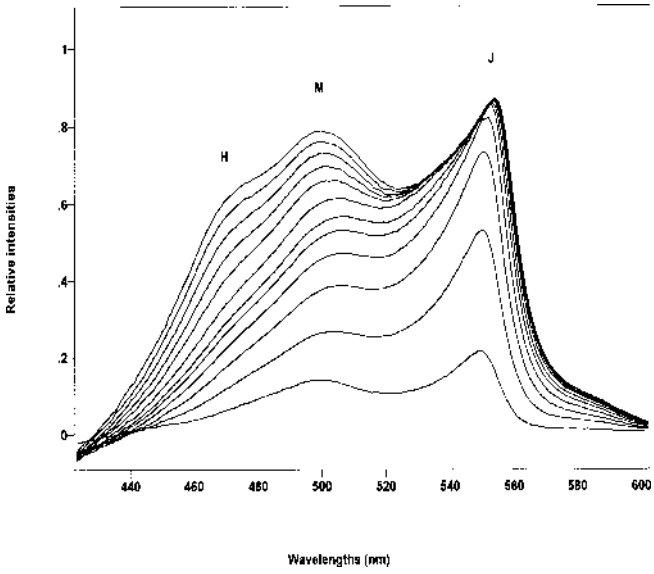

Figure 5. Visible absorption spectra of the spectrally sensitized emulsion as a function of dye coverage. From the top to the bottom, dye coverages are, respectively: 200, 180, 160, 140, 120, 110, 100, 90, 80, 50, 30, and 10% of a monolayer.

molecular long axis. The angle between the molecular long axis and the line of centers of stacked molecules is less than 32°. Various structures were proposed for the J-aggregates: "staircase," "brickstone," or "ladder."[20]

As an example, we present the visible absorption spectra of the dye in dilute methanol solution, aqueous solution, and a dilute solution of Na_2SO_4(Fig. 3). These spectra were obtained using a Perkin Elmer Lambda 9 UV-Visible spectrophotometer,Perkin Elmer Corp., Norwalk, CT. The spectral changes have been attributed to aggregation of the dye molecules in solution to form dimers and higher size aggregates under the influence of the dielectric constant or the nature and the polarity of the solvent.[21] The monomer has been called M and is characterized by an M-absorption band located at λ = 500 nm. The other species, dimer and trimer, are called H-aggregates and present an H-absorption band at λ = 465 nm.

The absorption spectrum of the adsorbed dye is similar to the one obtained in ionic solution where we observe so-called J-aggregates with the J-band shifted to a higher wavelength: λ = 550 nm.

Study as a Function of Dye Coverage. The first set of experiments was conducted on spectrally sensitized tabular grains by varying the amount of dye adsorbed on the grain surface (grain coverage varying from 0 to 80% of a theoretical monolayer). Both AFM and PSTM measurements were performed on samples of a spectrally

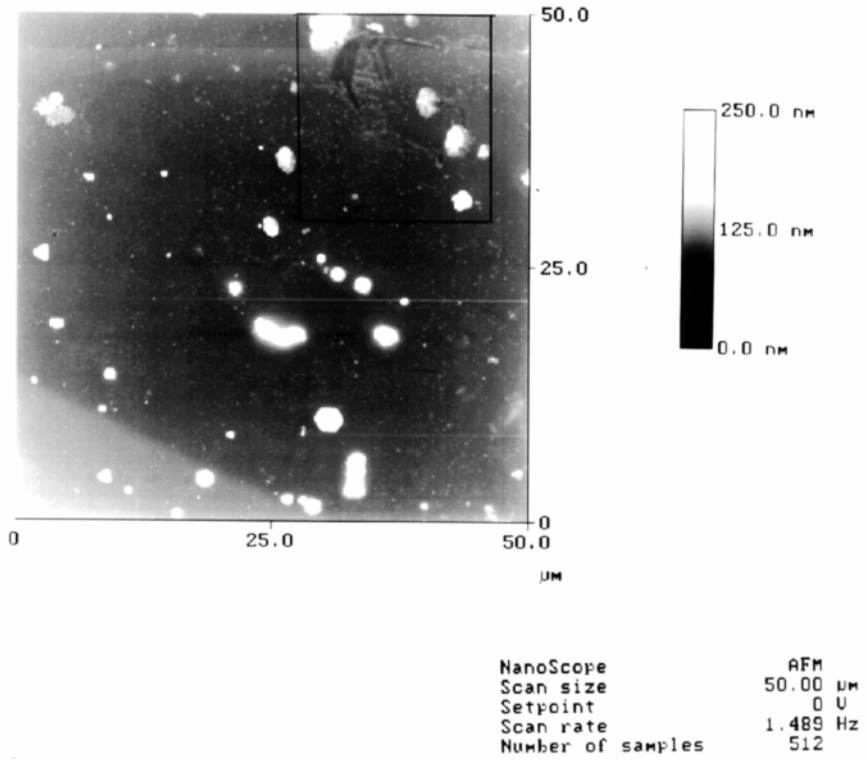

Figure 6. AFM image of the reference sample consisting in nonsensitized tabular grains. The scanning range is 50 × 50 µm. The image is performed in the contact mode. The area observed with the PSTM (Fig. 7) corresponds to the black square.

sensitized emulsion by means of the elaborated localization method. The PSTM images were recorded using red excitation to avoid photolysis. In that case, we observed an increase of the apparent height of the grains (from 130 to 350 nm) as a function of dye coverage (Fig. 4) on the PSTM images, while the height of the same grains measured by AFM remained almost constant (from 130 to 170 nm).

The apparent height increased up to a coverage corresponding to approximately 50% of a theoretical monolayer, which is close to what we observed on a macroscopic scale. We measured the visible absorption spectra of the adsorbed dye (Fig. 5) for dye coverage varying from 0 to 200% of a monolayer using the pure emulsion as a reference for the background. The intensity of the J-band increases with increasing dye coverage and reaches a limit for a dye coverage of 80% of a monolayer. This saturation corresponds to the formation of an "efficient" monolayer of dye molecules.

For dye coverage higher than 80%, the observed increase of the M-band is due to the adsorption of dye monomers on top of this monolayer and in the gelatine surrounding the grains.

The increase in grain height may be explained by either the real increase of the thickness of the tabular grain due to the presence of a monolayer of dye molecules or the optical contribution of this monolayer of dye molecules adsorbed to the grain surface (variations of the refractive index, fluorescence).

The average thickness of spectrally sensitized tabular grains observed with AFM was about 170 nm, from 15 to 80% of dye coverage. The average thickness of nonsensitized grains has been previously established to 130 nm. The AFM technique providing topographical information of high quality allows us to conclude that the nominal thickness of the dye monolayer and the gelatine is about 40 nm. This value is in good agreement with the value previously evaluated by Maskasky[22] to 20 nm. However, this is not a real height increase but a combination of the change of the dimensional parameters and the forces between the tip and the sample. When the dye adsorption increases, the tip probably starts to interact with the dye instead of the pure gelatine adsorbed on the grains.

In the case of PSTM, the changes in the z direction are much higher than for AFM. This is due to the optical contribution of the monolayer of dye molecules to the intensity of the light recorded with the PSTM technique. The cyanine dye molecules are known to present fluorescence properties.

Study with Both AFM and PSTM of Spectrally Sensitized Tabular Grains at Various Excitation Wavelengths. To further investigate the spectroscopic ability of our system, we carried out a different set of PSTM experiments where the amount of dye remained constant but the excitation wavelength was changed from the red (632.8 nm) to the green (514.5 nm) with several steps to obtain an emission profile of the dye on the grain.

The excitation wavelengths were chosen to cover the range of absorption of the sensitizing dye. For this study, we first examined a reference sample made of nonsensitized emulsion and then two spectrally sensitized emulsion samples with two dye coverages: 15% (sample B) and 50% (sample A).

Figure 6 presents the AFM image of a nonsensitized emulsion sample performed using the contact mode with a scanning range of 50 × 50 µm.

The area observed with PSTM corresponds to the black square (20 × 20 µm). The first PSTM image was performed at λ = 632.8 nm [Fig. 7(a)] and the following images were obtained for various wavelengths contained in the absorption range of the dye [Figs. 7(b) and 7(c)]. The last image [Fig. 7(d)] was done at λ = 632.8 nm to verify that the sample did not change during the experiment and no mechanical drift occurred. Each set of images was rapidly performed to avoid the photolysis of the grains.

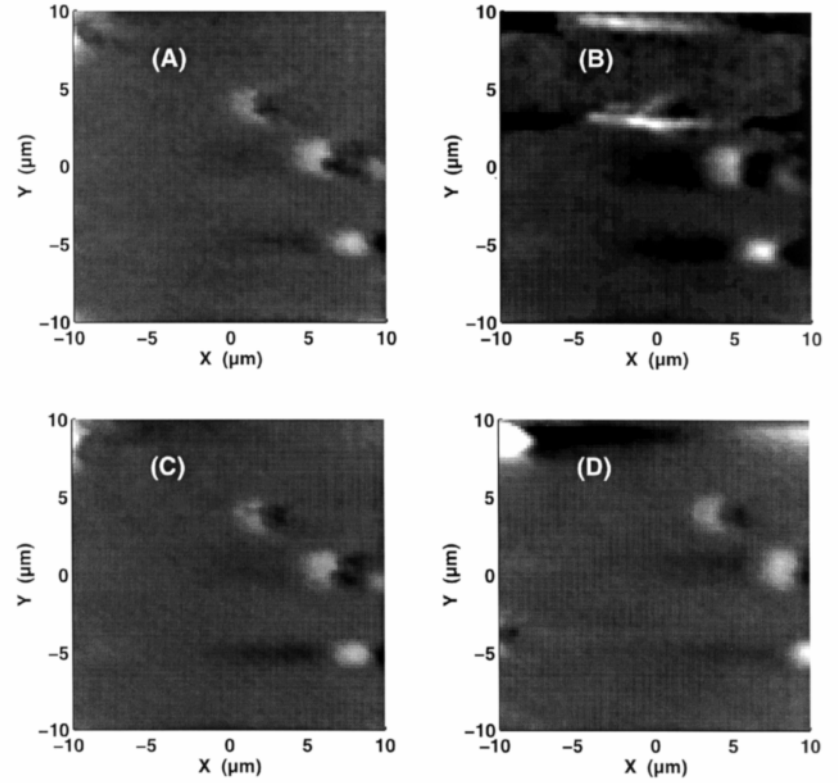

Figure 7. PSTM images of the reference sample performed at various excitation wavelengths in constant intensity mode of imaging with an incoherent xenon lamp source. The scanning range is 20×20 μm and the angle of incidence 60°. The gray scale ranges from 0 to 200 nm: (a) $\lambda_1 = 632.8$ nm; (b) $\lambda_2 = 514.5$ nm; (c) $\lambda_3 = 550$ nm; (d) $\lambda_4 = 632.8$ nm.

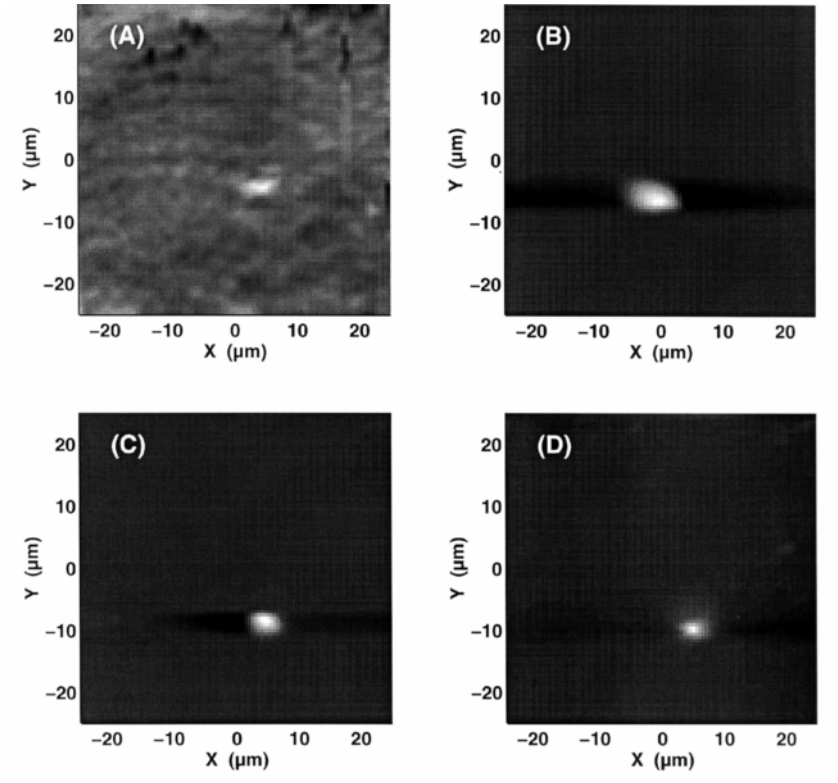

Figure 8. PSTM images of the spectrally sensitized sample: sample A (50% of surface coverage) performed at various excitation wavelengths with an angle of incidence of 60°. The source used is an incoherent xenon lamp with S polarization. The scanning range is 50×50 μm and the scanning time 1 min: (a) $\lambda_1 = 632.8$ nm.The gray scale ranges from 0 to 350 nm; (b) $\lambda_2 = 514.5$ nm. The gray scale ranges from 0 to 3500 nm; (c) $\lambda_3 = 550$ nm. The gray scale ranges from 0 to 2750 nm; (d) $\lambda_4 = 632.8$ nm. The gray scale ranges from 0 to 350 nm.

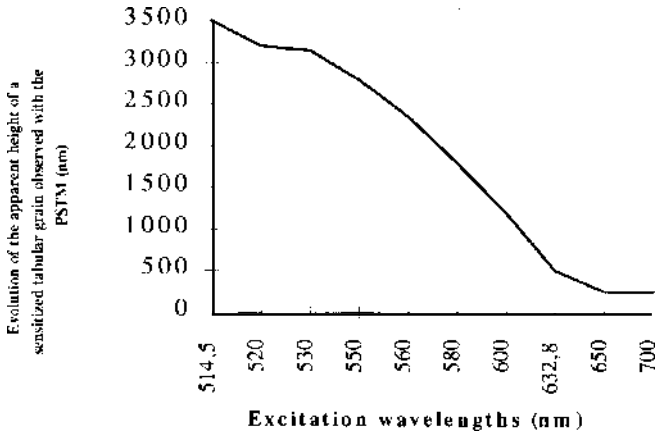

Figure 9. Evolution of the apparent thickness of the tabular grain observed with PSTM as a function of excitation wavelength.

The scanning time was about 100 s for each PSTM image. No difference was noticed on the PSTM images as a function of the excitation wavelengths. This reference sample allowed us to conclude that no differential effect existed on the PSTM images in the absence of dye molecules adsorbed to the surface of the grain.

We, then, investigated a sample with high dye coverage (50%) but that did not reach the theoretical monolayer. The area (50×50 μm) observed with the PSTM contained a single microcrystal with hexagonal shape established by classical optical microscopy and AFM techniques. Figures 8(a) to 8(d) present the PSTM images of the sample (called sample A) performed at various excitation wavelengths: 632.8, 514.5, 550, and 632.8 nm with a xenon incoherent source and using the constant-intensity mode of imaging. The scanning time was about 1 minute for each image.

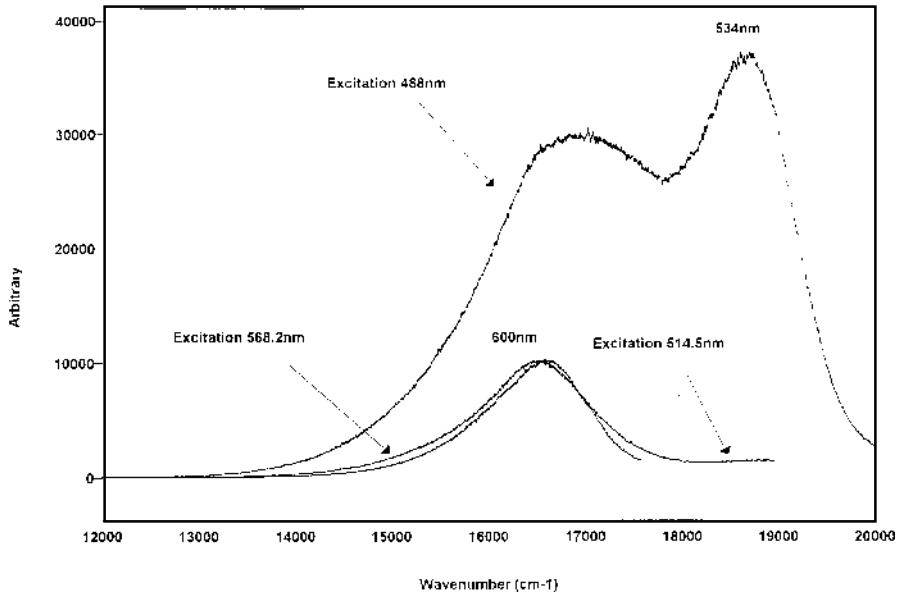

Figure 10. Fluorescence emission spectra of the pure sensitizing dye at room temperature. The excitation wavelengths are, respectively: 488, 514.5, and 568.2 nm.

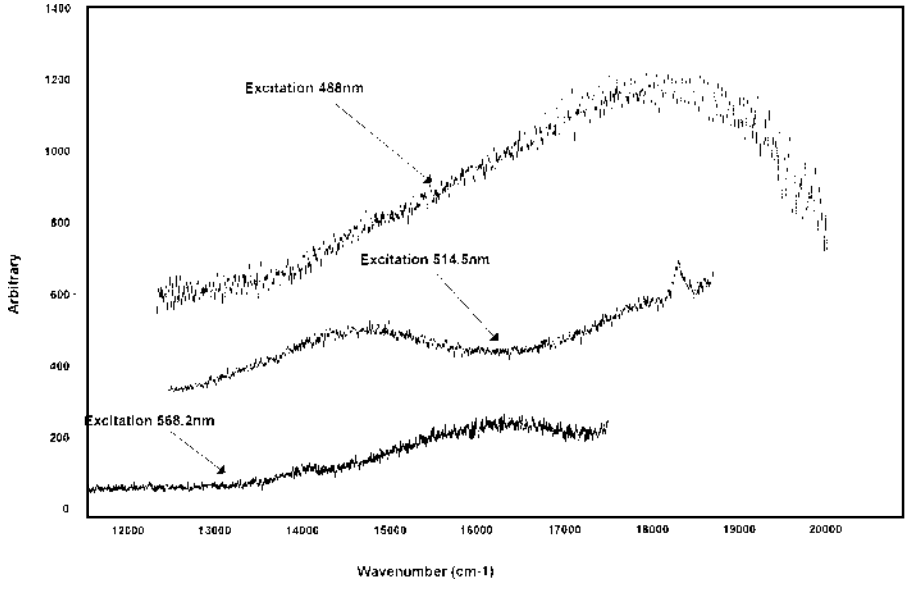

Figure 11. Fluorescence emission spectra of the adsorbed dye at room temperature. The excitation wavelengths are, respectively: 488, 514.5, and 568.2 nm.

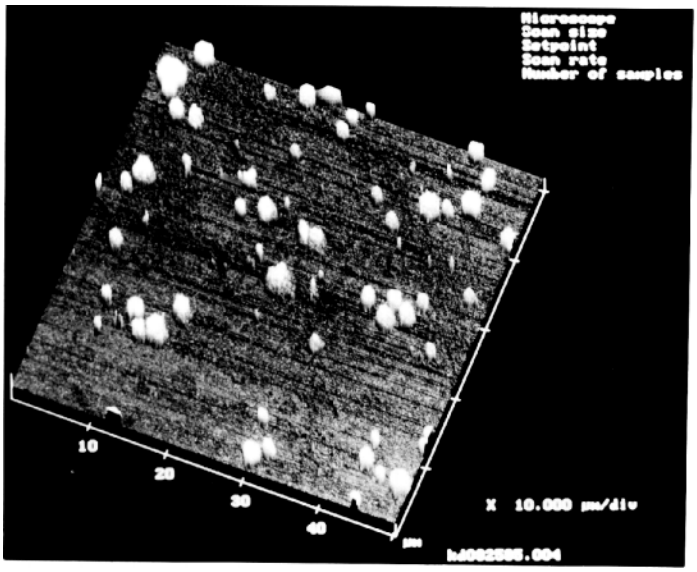

Figure 12. AFM image of the spectrally sensitized emulsion sample with a surface coverage of 5% (sample B) with sensitizing dye. The mode of imaging used was the contact mode. The scanning range was 50 × 50 μm.

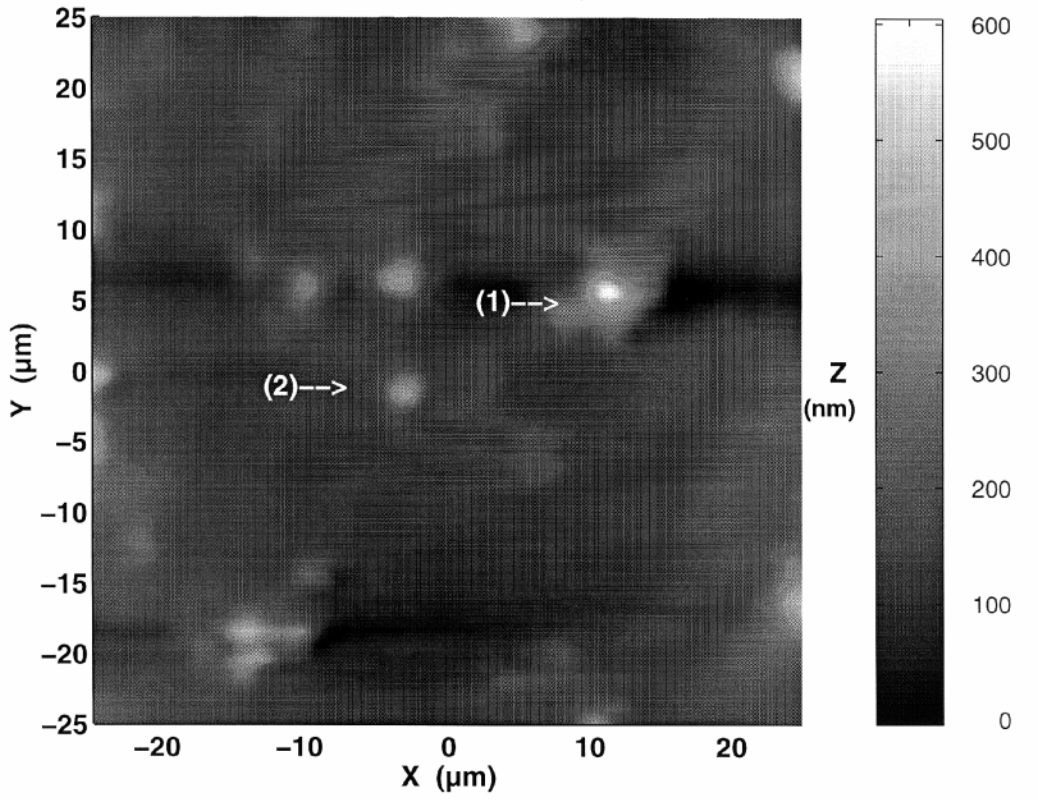

Figure 13. PSTM image of the same area of sample B (5% of dye coverage). The scanning range was 50 × 50 μm, the excitation wavelength 632.8 nm, the angle of incidence 60°, and we used the constant intensity mode of imaging.

The apparent height of the sample for each measurement is reported in Fig. 9 as a function of the excitation wavelength (one measurement every 10 nm from 520 to 600 nm reproduced on more than 10 sample areas). The shape of the curve is similar to the absorption spectrum of the dye adsorbed on the grain with a maximum around 560 nm. For $\lambda = 514.5$ nm, the apparent thickness of the grain was 3.5 μm and the apparent diameter 8 μm. This height decreased as a function of the excitation wavelength and reached a value of 200 nm for $\lambda = 632.8$ nm (outside the absorption range of the dye). This value is in good agreement with the values obtained in the Fig. 5.

To verify the hypothesis that the phenomenon is related to the fluorescence of the sensitizing dye adsorbed to the tabular grains, we collected the fluorescence spectra of this dye at room temperature. The fluorescence spectra were performed on a DILOR XY Raman spectrophotometer, Lille, France, with different excitation wavelengths selected in the absorption range of the sensitizing dye.

Figure 10 gives an example of fluorescence spectra of pure dye obtained for various excitation wavelengths: 488, 514.5, and 568.2 nm. No fluorescence was detected for an excitation at 647.1 nm, but we observed the Raman spectrum of the sensitizing dye.

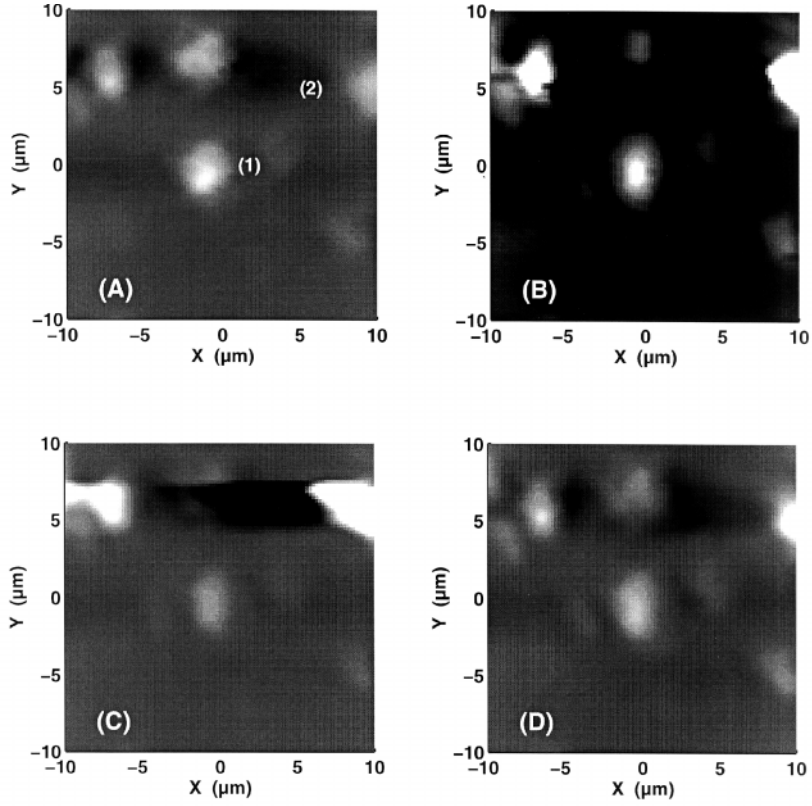

Figure 14. PSTM images of the spectrally sensitized emulsion sample: sample B (5% of dye coverage) performed at various excitation wavelengths with a incoherent xenon lamp source: 632.8, 514.5, 550, and 632.8 nm. The scanning range was 20×20 µm, the angle of incidence 60°, and we used the constant intensity mode of imaging. (a) $\lambda_1 = 632.8$ nm. The color scale ranges from 0 to 200 nm; (b) $\lambda_2 = 514.5$ nm. The color scale ranges from 0 to 800 nm; (c) $\lambda_3 = 550$ nm. The color scale ranges from 0 to 900 nm; (d) $\lambda_4 = 632.8$ nm. The color scale ranges from 0 to 180 nm.

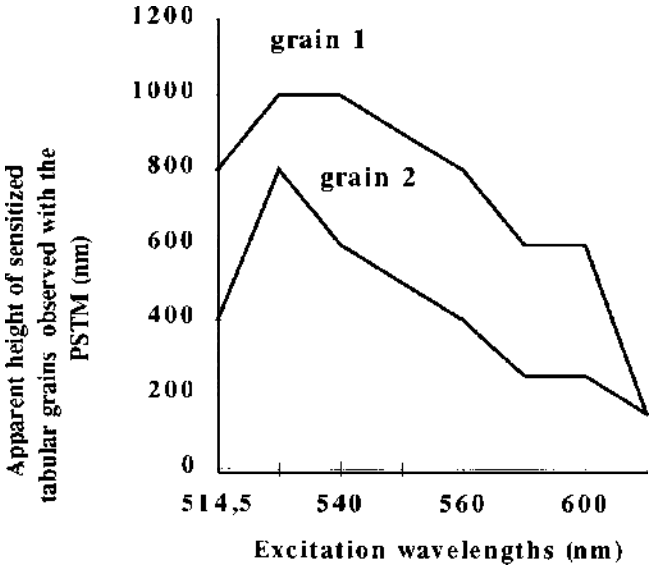

Figure 15. Evolution of the apparent thickness of the spectrally sensitized emulsion grains (5% of dye coverage) observed with PSTM as a function of the excitation wavelengths: 1 is a group of several grains, 2 corresponds to a single hexagonal microcrystal.

Figure 11 presents the fluorescence emission of the dye adsorbed on the tabular grain emulsion for a dye coverage of 50%. The intensity of the signal decreased by a factor of 50 compared to the signal of the pure dye because of the adsorption of the dye on the grain surface.

The emission appears only for the excitation wavelengths within the absorption range of the dye (488 to 568.2 nm). The appearance of these spectra is very similar to the spectra collected on the pure dye but are slightly shifted to higher wavelengths. The two experiments prove that collecting fluorescence information related to the dye chosen is possible even in the case of adsorbed dye at room temperature. In other words, increase of the apparent thickness of microcrystals, observed with the PSTM technique, corresponds to the dye fluorescence.

The last image performed at $\lambda = 514.5$ nm after the sets of images [Figures 8(a) to 8(d)] showed an amplification of the apparent thickness as important as the amplification observed at the beginning of the experiment. The grain had not yet undergone the complete effect of the photolysis. We showed that it was possible to observe the fluorescence phenomenon in the near-field for the AgBr spectrally sensitized grain with the PSTM technique by varying the excitation wavelengths. Experiments with classical fluorescence optical microscopy conducted on spectrally sensitized emulsion samples (50% of dye coverage) revealed a fluorescence response for an excitation wavelength at $\lambda = 450$ nm. These experiments confirmed that the used sensitizing dye fluoresces and that the fluorescence signal is observable for several minutes.

To complete this study, we performed the same experiments using a sample with low dye coverage: 5% (sample B). The spatial localization of the tabular microcrystals was feasible with the image obtained with AFM (Fig. 12) on a area of 50×50 μm. The corresponding PSTM image is presented in Fig. 13. The studied area presents a particular arrangement with a single hexagonal microcrystal (grain 2) at the center of the image and a group of five hexagonal grains (grain 1) to the right of the area.

We were interested in the possible difference between the fluorescence behavior of the isolated grain and that of the group of grains.

The comparison between the PSTM and AFM image was easily done. It showed that the group of five grains was not separated on the PSTM image. On the following images [Figs. 14(a) to 14(d)] performed at various excitation wavelengths, the scanning time was about 50 to 100 s, which was a small value in comparison with the ones currently used with the NSOM technique (about 20 min). The curves corresponding to the single grain 2 and to the group of grains 1 are showed in Fig. 15 summarizing the evolution of the apparent thickness of the spectrally sensitized microcrystals (5% of dye coverage) detected with PSTM as a function of the excitation wavelength.

As in the case of high dye coverage (50%), the increase of the apparent thickness of the spectrally sensitized grains occurred for the excitation wavelengths contained in the absorption range of the sensitizing dye.

Note that the height increase for the group of grains 1 is more important than the increase observed for the single grain and that the appearance of curve 1 is slightly different than the appearance of the similar curve obtained with sample A. The difference between 1 and 2 could be due to inhomogeneity of the dye coverage between one grain and another. The fluorescence response of the spectrally sensitized grains detected by classical fluorescence optical microscopy shows heterogeneous response especially if the dye coverage is low or if the grains are isolated or packed.

The second effect noticed is the difference between sample A and B and especially the appearance of the curve for the excitation wavelength at 514.5 nm. The PSTM response associated to the fluorescence of the sample B began with a lower intensity than the response associated to sample A. We assume this is due to the existence of different forms of dye aggregates as a function of the dye coverage.

For low dye coverage, the J-aggregates are dominant while for high dye coverage it is possible to find monomers or H-aggregates adsorbed on the grain or in the gelatine near the grains. These later species absorb at a lower wavelength than the J-aggregates and could explain the higher response at 514.5 nm excitation in the case of high dye coverage (sample A).

Conclusions

We showed that the combination of AFM and PSTM information allows us to measure the differences between spectrally sensitized and nonsensitized microcrystals. This direct comparison between AFM and PSTM images of the same microcrystals was only possible with the localization method using a carbon coating developed in our laboratory. We observed an increase of the apparent thickness of the spectrally sensitized grains as a function of the dye coverage only in the case of the PSTM images. The AFM images did not allow us to detect the optical contribution of the monolayer of dye molecules adsorbed on the tabular grain surface.

PSTM images performed at various excitation wavelengths confirmed the existence of an important amplification of the apparent height of the grains for the excitation wavelengths corresponding to the absorption range of the sensitizing dye. The "macroscopic" fluorescence experiments performed at room temperature confirmed the existence of fluorescence emission detectable during a few minutes for excitation wavelengths contained in the absorption range of the dye.

The evolution of the grains apparent thickness observed with PSTM as a function of the excitation wavelengths are different for high dye and low dye coverage. This phenomenon has also been observed with classical fluorescence optical microscopy, and we assume this is due to the existence of different forms of aggregates on the grains as a function of dye coverage.

These recent developments coupling the AFM topographical ability with the PSTM spectroscopic information open new routes for better understanding of the addenda adsorption mechanisms and better characterization of the photographic emulsion.

To improve these experiments, we plan to analyze spectrally the signal collected by the optical fiber tip. The interest is the possible quantification and selection of the information collected by the tip for the measurements performed at various excitation wavelengths. Another parameter important to take into account in a further study is the polarization of the incident beam as a function of the orientation of the adsorbed dye molecules.

Acknowledgments. We wish to thank E. Lesniewska and E. Bourillot for performing an important part of the AFM measurements and C. Legrimellec for providing the fluorescence optical microscopy images of sensitized tabular grains.

References

1. J. E. Maskasky, *J. Imag. Sci. Technol.* **31,** 15 (1987).
2. J. E. Maskasky, *J. Imag. Sci. Technol.* **32,** 15 (1988).
3. J. E. Maskasky, *J. Imag. Sci. Technol.* **35,** 29 (1991).
4. D. A. Vandenbrouke, *J. Inf. Rec. Mats. Technol.* **20,** 517 (1993).
5. H. Saijo, T. Isshiki, M. Shiojiri, G. Ning, and K. Ogawa, *J. Imag. Sci. Technol.* **38,** 217 (1994).
6. E. Meyer, H. J. Güntherodt, H. Haefke, G. Gerth, and M. Krohn, *Europhys. Lett.* **15,** 319 (1991).
7. G. Hegenbart and Th. Mussig, *Surf. Sci. Lett.* **275,** L655 (1992).
8. H. Takada and H. Nozoye, *Langmuir* **9,** 3305 (1993).
9. H. Haefke, U. D Schwarz, H. J. Güntherodt, H. Föb, G. Gerth, and R. Steiger, *J. Imag. Sci. Technol.* **37,** 545 (1993).
10. H. Saijo, M. Shiojiri, S. Watanabe, and T. Tani, in *Proc. IS&T'S 48th Annual Conference,* IS&T, Springfield, VA, 1995, p. 215.
11. H. Saijo, M. Shiojiri, S. Watanabe, and T. Tani, in *Proc. IS&T'S 49th Annual Conference,* IS&T, Springfield, VA, 1996, p. 207–212.
12. M. Kawasaki and H. Ishii, *J. Imag. Sci. Technol.* **39,** 210 (1995).
13. J. K. Rogers, R. Toledo-Crow, M. Vaez-Iravani, G. Di Francesco, T. Zhao, and R. Hailstone. *J. Imag. Sci. Technol.* **39,** 205 (1995).
14. R. C. Reddick, R. J Warmack, and T. L Ferrell, *Phys. Rev. B* **39,** 767 (1989).
15. F. De Fornel, J. P. Goudonnet, L. Salomon, and E. Lesniewska, in *Proc. SPIE* **1139,** 77, (1989).
16. D. Courjon, K. Sarayeddine, and M. Spajer, *Opt. Commun.* **71,** 23 (1989).
17. E. E. Jelley, *Nature* **138,** 1009 (1936).
18. S. Dahne, *J. Imag. Sci. Technol.* **38,** 101 (1994).
19. W. West and P. Gilman, in *Theory of the Photographic Process,* 4th ed, T. H James, Ed. Macmillan, New York, 1977, Chap. 10.
20. V. Czikkely, H. D. Forsterling, and H. Kuhn, *Chem. Phys. Lett.* **6,** 11 (1970).
21. A. H. Hertz, *Photogr. Sci. Eng.* **18,** 323 (1974).
22. J. E. Maskasky, *J. Imag. Sci.* **32,** 160 (1988).